JOURNAL OF THERMOPHYSICS AND HEAT TRANSFER
Vol. 6, No. 2, April–June 1992

Thermal Contacts in Transient States: A New Model and Two Experiments

Alain Degiovanni,* Anne-Sophie Lamine,† and Christian Moyne‡
Unité de Recherche Associée, 54504 Nancy, France

In the present paper a model of thermal contact in transient state using the notion of "thermal quadripoles" is presented. This model takes into account two particular aspects of the transient state: the establishment of the heat flow lines and the heat capacities of both contact spots and interstitial fluid. Two experiments in steady periodical state are shown: one deals with real contacts, whereas the other concerns a macro-contact. The latter shows good qualitative agreement with the proposed model. In the real contact case, satisfactory agreement is obtained for the 0–0.02 Hz frequency range; for the 0.02–0.1 Hz range, differences are observed and stay yet unexplained.

Nomenclature

a	=	heat diffusivity
A, B, C, D	=	quadripole coefficients
A_n	=	coefficient [see Eq. (16)]
F_n	=	coefficients [see Eq. (18)]
f	=	frequency
J_0, J_1	=	Bessel functions of order 0 and 1
k	=	Laplace parameter ($= \sqrt{p/a}$)
L	=	thickness
p	=	Laplace variable
q	=	heat flux density
r, R	=	radius
R_c	=	constriction resistance per unit area
r_c	=	constriction resistance
r_0	=	spot radius
$r_{(t)}$	=	(thermal) resistance
S	=	cross-sectional area
s	=	cross section of the contact spot
T	=	temperature
t	=	time
x	=	space coordinate
Z_c	=	constriction impedance per unit area
z_c	=	constriction impedance
α_n	=	roots of transcendent equation $J_1(\alpha_n R) = 0$
λ_n	=	coefficients [see Eq. (16)]
δ	=	thickness of the contact spot
θ	=	Laplace transform of the temperature
φ	=	Laplace transform of the heat flux density or phase angle
Φ	=	Laplace transform of the flux
λ	=	heat conductivity

Subscripts

a	=	contact spot
f	=	fluid
s	=	solid

Superscript

$-$	=	average

Presented as Paper 90-0542 at the AIAA 28th Aerospace Sciences Meeting, Reno, NV, Jan. 8–11, 1990; received June 22, 1990; revision received April 21, 1991; accepted for publication April 28, 1991.

*Professor, Laboratoire d'Energetique et de Mecanique Theorique et Appliquee, C.N.R.S. 875-2, Avenue de la Foret de Haye, B.P. 160.

†Maître de Conférences, Laboratoire d/Energetique et de Mecanique Theorique et Appliquee; currently at Ecole nationale supérieure des Industries Chimiques, Laboratoire des Sciences du Génie Chimique, 1 rue Grandville, 54042 Nancy, France. Member AIAA.

‡Chargé de Recherche, Laboratoire d'Energetique et de Mecanique Theorique et Appliquee, C.N.R.S. 875-2, Avenue de la Foret de Haye, B.P. 160.

I. Introduction

A GREAT number of theoretical and experimental studies have been carried out on thermal contacts in steady-state conditions,[1–4] but little has been done in transient regimes where difficulties arise at both the theoretical and experimental level.

A bibliographic search for works in the transient case[5] shows that no precise study has been made of the time variation of the constrictions.

II. Model of Thermal Contact in Transient State

A. Notion of a Thermal Quadripole

A plane layer in steady-state conditions reduces to a thermal resistance. In the same manner, the layer in transient state conditions may be strictly modeled by a thermal quadripole which links Laplace transforms of input (subscript 1) and output (subscript 2) temperatures (θ) and heat fluxes (Φ) (see Fig. 1).

One can use, for example, the matrix notation

$$\begin{pmatrix}\theta_1\\ \Phi_1\end{pmatrix} = \begin{pmatrix}A & B\\ C & D\end{pmatrix}\begin{pmatrix}\theta_2\\ \Phi_2\end{pmatrix} \tag{1}$$

where

$$\begin{pmatrix}A & B\\ C & D\end{pmatrix}$$

denotes the inverse transfer matrix and $A = D = \cosh(k\,L)$; $C = \lambda k S \sinh(k\,L)$; $B = (A\,D - 1)/C$, where $k = \sqrt{p/a}$ (with p = Laplace variable); L = wall thickness; a = wall diffusivity; S = wall cross-sectional area; and λ = wall heat conductivity.

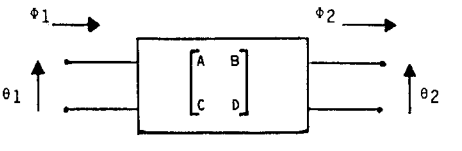

Fig. 1 Thermal quadripole of a "wall."

B. Thermal Quadripole Related to a Constriction

It is well known that in steady-state conditions, the notion of thermal resistance can only be used rigorously in particular systems composed of a heat flux pipe limited by two isothermal surfaces (see Fig. 2a).

Nevertheless, in the case where the surfaces are not isothermal, one often defines,[6,7] the thermal resistance (r_t) by

$$\bar{T}_1 - \bar{T}_2 = r_t \int_{S_1} q \, dS \tag{2}$$

where $\bar{T}_1$, $\bar{T}_2$ are the average temperatures of surfaces S_1 and S_2, and q the local heat flux density on surface S_1. In this case, the thermal resistance is not an intrinsic property of the medium and depends on the boundary conditions on S_1 and S_2.

The same generalization is used in transient state conditions. To make this approach more explicit, the elementary heat flux pipe of Fig. 2b is studied here. The temperature field is the solution of the following system:

$$\frac{\partial^2 T}{\partial x^2} + \frac{1}{r}\frac{\partial T}{\partial r} + \frac{\partial^2 T}{\partial r^2} = \frac{1}{a}\frac{\partial T}{\partial t} \tag{3}$$

$$\text{for } r = R \qquad \frac{\partial T}{\partial r} = 0 \tag{4}$$

$$\text{for } x = L - \lambda \frac{\partial T}{\partial x} = q(r, t) \quad \text{if } 0 < r < r_0 \tag{5}$$

$$\text{if } r_0 < r < R$$

$$\text{for } x = 0 \text{ Any boundary condition independent of } r \tag{6}$$

$$t = 0 \qquad T = 0 \tag{7}$$

As well as in Sec. II.A., a quadripole can be associated to this problem:

$$\bar{\theta}_1 = A\bar{\theta}_2 + B\Phi_2 \tag{8}$$

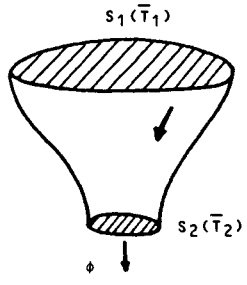

a) $r_t = (\bar{T}_1 - \bar{T}_2)/\Phi$

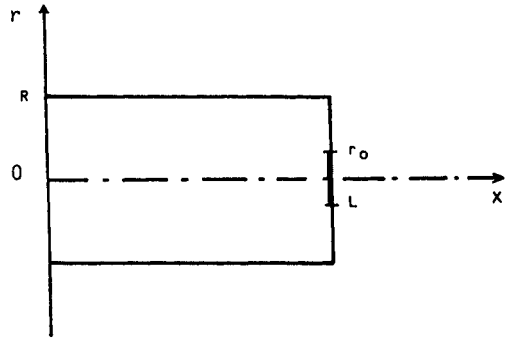

b) constriction model

Fig. 2 Heat flux pipe.

$$\Phi_1 = C\bar{\theta}_2 + D\Phi_2 \tag{9}$$

where

$$\bar{\theta}_1 = \frac{2}{R_2}\int_0^R \theta_{x=0}\, r\, dr \tag{10}$$

$$\bar{\theta}_2 = \frac{2}{r_0^2}\int_0^{r_0} \theta_{x=L}\, r\, dr \tag{11}$$

$$\Phi_1 = 2\pi \int_0^R \left(-\lambda \frac{\partial \theta}{\partial x}\right)_{x=0} r\, dr \tag{12}$$

$$\Phi_2 = 2\pi \int_0^{r_0} \left(-\lambda \frac{\partial \theta}{\partial x}\right)_{x=L} r\, dr \tag{13}$$

In our notation, θ denotes the Laplace transform of temperature T. As in steady-state conditions, the terms A, B, C, D, depend on the boundary conditions at $x = 0$ and $x = L$. In fact, whenever the medium is assumed sufficiently thick, the type of condition at $x = 0$ does not modify heat transfer. As shall be proved later, the condition ($L > R$), which is always verified in practice, is sufficient. Therefore (for $L > R$), the quadripole becomes an intrinsic property of the medium and each term of the transfer matrix is independent of the boundary conditions and can be calculated separately. Of course the same problem appears at $x = L$ but a preceding study[8] has shown the weak influence of the boundary condition [Eq. (5)].

It is then possible to calculate the terms of the quadripole by choosing convenient conditions at $x = 0$.

For $\bar{\theta}_1 = 0$

$$B = -\bar{\theta}_2/\Phi_1 \quad \text{and} \quad A = \Phi_2/\Phi_1 \tag{14}$$

For $\Phi_1 = 0$

$$D = \bar{\theta}_2/\bar{\theta}_1 \quad \text{and} \quad C = \Phi_2/\bar{\theta}_1 \tag{15}$$

The system (3)–(7) may then be solved using particular boundary conditions at $x = 0$. The conditions $T = 0$ and $\partial T/\partial x = 0$ are chosen here.

For both conditions, an analytical solution is obtained by applying Laplace transform on time, and separating the space coordinates.

For the first condition, the general solution of Eq. (3–7), is

$$\theta(x, r) = A_0 \sinh(kx) + \sum_{n=1}^{\infty} A_n J_0(\alpha_n r) \sinh(\gamma_n x) \tag{16}$$

with

$$A_0 = \frac{2\int_0^{r_0} r\varphi(r)\, dr}{-\lambda k \cosh(kL) R^2}$$

$$A_n = \frac{2\int_0^{r_0} r\varphi(r)\, J_0(\alpha_n r)\, dr}{-\lambda \gamma_n \cosh(\gamma_n L) R^2 J_0^2(\alpha_n R)}$$

where $k = \sqrt{p/a}$; $\varphi(r)$ is the Laplace transform of the local heat flux density $q(r, t)$; J_0 and J_1 are Bessel functions of order 0 and 1; $(\alpha_n R)$ are the roots of $J_1(\alpha_n R) = 0$; $\gamma_n^2 = \alpha_n^2 + k^2$. The terms A and B are derived using Eq. (14).

For the second condition, the general solution of Eqs. (3–7) is found by changing the "cosh" for "sinh" and conversely, applying Eq. (15) yields the expressions of terms D and C.

Hence, the final expressions of the quadripole terms are

$$A = \cosh(kL) \tag{17}$$

$$B = \sinh(kL)/(\pi R^2 \lambda k) + \sum_{n=1}^{\infty} F_n \cosh(kL) \tanh(\gamma_n L) \tag{18}$$

$$C = \pi R^2 \lambda k \sinh(kL) \tag{19}$$

$$D = \cosh(kL) + \sum_{n=1}^{\infty} F_n \pi R^2 \lambda k \sinh(kL) \operatorname{cotanh}(\lambda_n L) \tag{20}$$

with

$$F_n = \frac{2 J_1(\alpha_n r_0) \int_0^{r_0} r\varphi(r) J_0(\alpha_n r)\, dr}{\pi \lambda \alpha_n r_0 R^2 \gamma_n J_0^2(\alpha_n R) \int_0^{r_0} r\varphi(r)\, dr} \tag{21}$$

The equation $(A\,D - B\,C = 1)$, which is characteristic of a passive quadripole, is only verified if

$$\tanh(\gamma_n L) \simeq \operatorname{cotanh}(\gamma_n L) \simeq 1 \tag{22}$$

As the first zero of J_1 is $j_{1,1} \simeq 3.83$, condition (22) is fulfilled as soon as L/R is greater than 1 ($\tanh(j_{1,1}) \simeq 0.999$). Furthermore, the most restrictive condition, since $\gamma_n^2 = \alpha_n^2 + p/a$, is obtained for $p = 0$, that is to say in the steady-state regime.

In that case, the above quadripole appears to be the product of two quadripoles, the first being related to the unperturbed medium of thickness L (the "wall"), whereas the second one is characteristic of the constriction of the heat flux lines

$$\begin{bmatrix} A & B \\ C & D \end{bmatrix} = \begin{bmatrix} A' & B' \\ C' & D' \end{bmatrix} \begin{bmatrix} A'' & B'' \\ C'' & D'' \end{bmatrix} \tag{23}$$

with

$$\begin{cases} A' = D' = \cosh(k\,L) \\ C' = \pi R^2\, \lambda k \sinh(k\,L) \\ B' = (A'\,D' - 1)/C' \end{cases}$$

and

$$\begin{cases} A'' = D'' = 1 \\ C'' = 0 \\ B'' = \sum_{n=1}^{\infty} F_n = z_c \end{cases}$$

The quadripole associated with the constriction of the heat flux lines appears as an impedance (z_c) since it has the following form:

$$\begin{bmatrix} 1 & z_c \\ 0 & 1 \end{bmatrix} \tag{24}$$

This very general result may be extended to other geometrical shapes (cylinders with square or rectangular base for example) and to the particular case of steady periodical conditions using the complex notation and substituting p for $(2\pi f i)$.

For example, when the cell radius R is larger than the contact spot radius r_0, the expression of the impedance z_c may be found assuming that heat is supplied at $x = L$ with an uniform rate $q(t)$ over the circular area of radius r_0. The demonstration is given in the Appendix. The impedance z_c is given by

$$z_c = \frac{2}{\pi \lambda r_0} \int_0^{\infty} \frac{J_1^2(\varepsilon)}{\varepsilon} \frac{1}{\sqrt{\varepsilon^2 + p\, r_0^2/a}}\, d\varepsilon \tag{25}$$

The constriction impedance z_c appears to be an increasing function of time from 0 to

$$r_c = \frac{2}{\pi \lambda r_0} \int_0^{\infty} \frac{J_1^2(\varepsilon)\, d\varepsilon}{\varepsilon^2} = \frac{8}{3\pi^2 \lambda r_0} \tag{26}$$

which is the value of the constriction resistance obtained in steady-state conditions.[9] This variation is characteristic of the spatial setting up of the constriction.

C. Model of Thermal Contact

The solid–solid contact is modeled by a great number of cylindrical unit cells (see Fig. 3a).

This problem has already been examined in steady-state conditions (Degiovanni and Moyne[8]). Beginning with an exact model, a simplified scheme, which is valid for realistic contact conditions, has been built and is shown in Fig. 3b. The only limitations are that the ratio of the cross section of the contact spot (s) to the cross section of the unit cell (S) is lower than 1% ($s/S < 0.01$) and that the thermal conductivity of the fluid λ_f is lower or equal to the solid conductivities λ_1 or λ_2. This simplified model shows that the fluid resistance r_f is in parallel

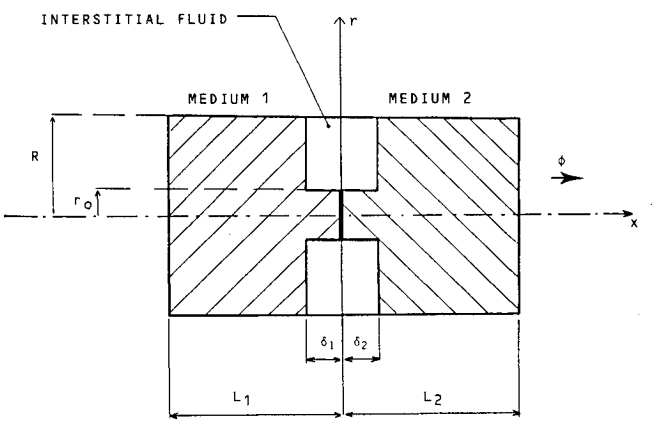

a) unit cell

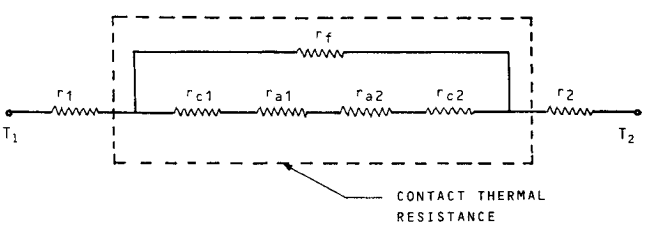

b) steady state

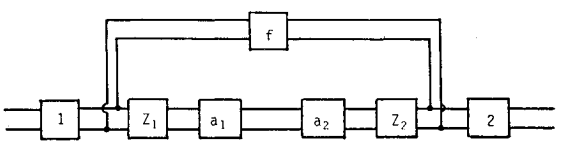

c) transient state

Fig. 3 Thermal contact.

with the resistance of the contact spot ($r_{a1} + r_{a2}$) in series with the constriction resistance ($r_{c1} + r_{c2}$).

This result is exact when fluid conductivity λ_f vanishes. When λ_f tends toward λ_s, then the fluid resistance r_f is much greater than the resistance of the contact spot in series with the constriction resistance ($r_f \ll r_{c1} + r_{a1} + r_{a2} + r_{c2}$). This is due to the fact that $s/S \ll 1$. Then the contact resistance is reduced only to the fluid resistance r_f.

The expressions of the resistances are:

1) unperturbed media 1 and 2

$$r_1 = \frac{L_1}{\lambda_1 S} \qquad r_2 = \frac{L_2}{\lambda_2 S} \tag{27}$$

2) fluid resistance

$$r_f = \frac{\delta_1 + \delta_2}{\lambda_f S} \tag{28}$$

3) contact spot

$$r_{a1} = \frac{\delta_1}{\lambda_1 S} \qquad r_{a2} = \frac{\delta_2}{\lambda_2 S} \tag{29}$$

4) constriction resistances

$$r_{c1} = \frac{K_1}{\lambda_1 \sqrt{\pi s}} \qquad r_{c2} = \frac{K_2}{\lambda_2 \sqrt{\pi s}} \tag{30}$$

where K_1 and K_2 are functions of the geometry of the unit cell (especially of the ratio s/S) and of the shape of the contact spot.

Using an analogy with the steady-state approach, the sketch on Fig. 3c is proposed for the transient state. In this sketch the "wall" resistances (r_1, r_2, r_f, r_{a1}, and r_{a2}) are replaced by "wall" quadripoles and the "constriction" resistances (r_{c1} and r_{c2}) by "constriction" quadripoles. This representation, obtained by analogy, may be demonstrated using long and tedious analytical calculations on the unit cell.

In Fig. 3c, quadripoles /1/, /2/, /f/, /a_1/, and /a_2/ are of "wall" type, thus

$$\begin{cases} A = D = \cosh(\sqrt{p/a_n}\, L_n) \\ C = S_n \lambda_n \sqrt{p/a_n} \sinh(\sqrt{p/a_n}\, L_n) \\ B = (A\,D - 1)/C \end{cases} \tag{31}$$

where

$$\begin{aligned} S_n &= S \quad \text{for} \quad /1/, /2/ \quad \text{and} \quad /f/ \\ &= s \quad \text{for} \quad /a_1/ \quad \text{and} \quad /a_2/ \\ \lambda_n &= \lambda_1 \quad \text{for} \quad /1/ \quad \text{and} \quad /a_1/ \\ &= \lambda_2 \quad \text{for} \quad /2/ \quad \text{and} \quad /a_2/ \\ &= \lambda_f \quad \text{for} \quad /f/ \\ a_n &= a_1 \quad \text{for} \quad /1/ \quad \text{and} \quad /a_1/ \\ &= a_2 \quad \text{for} \quad /2/ \quad \text{and} \quad /a_2/ \\ &= a_f \quad \text{for} \quad /f/ \\ L_n &= L_1 \quad \text{for} \quad /1/ \\ &= L_2 \quad \text{for} \quad /2/ \\ &= \delta_1 \quad \text{for} \quad /a_1/ \\ &= \delta_2 \quad \text{for} \quad /a_2/ \\ &= \delta_1 + \delta_2 \quad \text{for} \quad /f/ \end{aligned}$$

and quadripoles /z_1/ and /z_2/ are of "constriction" type, thus

$$\begin{cases} A = D = 1 \\ C = 0 \\ B = z_c \end{cases} \tag{32}$$

with z_c given by expressions (21) and (23), where

$$\begin{aligned} \lambda &= \lambda_1 \quad \text{for} \quad /z_1/ \\ &= \lambda_2 \quad \text{for} \quad /z_2/ \\ a &= a_1 \quad \text{for} \quad /z_1/ \\ &= a_2 \quad \text{for} \quad /z_2/ \end{aligned}$$

III. Experiments on Real Contacts

A solid–solid contact between two copper solids, whose contact spots areas can be varied, is studied. Other variable parameters are the imposed mechanical pressure at the contact joint and the pressure of the interstitial air.

The experimental device is made of a pile of two cylindrical samples connected to a heating element on one side and a regulated water-cooled box on the other side. Each sample is composed of a Bi_2Te_2 layer welded to two copper cylinders (see Fig. 4).

A. Experimental Setup

The experimental setup is composed of a pile of six media submitted to periodical thermal excitation (Fig. 4). The Bi_2Te_3 layer is used to measure the thermal signal before and behind the contact; a voltage difference builds up between the two copper parts, which is proportional to the temperature difference between the two sides of the Bi_2Te_3 layer. All contact joints are brazed with tin and so regarded as perfect with the exception of the one being studied (see Fig. 4, contact joint 3–4).

In order to allow a comparison between model and experiments, the temperatures differences $F_1 = T_1 - T_2$ and $F_2 = T_5 - T_6$ at the terminals of the Bi_2Te_3 layer are used. A computer program using the quadripoles method[10] calculates the temperatures amplitudes and phases) of the system. The contact joint 3–4 is modeled either by a pure resistance or by the quadripole described in Sec. II.C. The experimental and theoretical results are then compared on Figs. 5–7.

B. Experimental Results

The common characteristics of all experimental tests are:

1) The electrical power of the signal lies between 1 and 10 W.

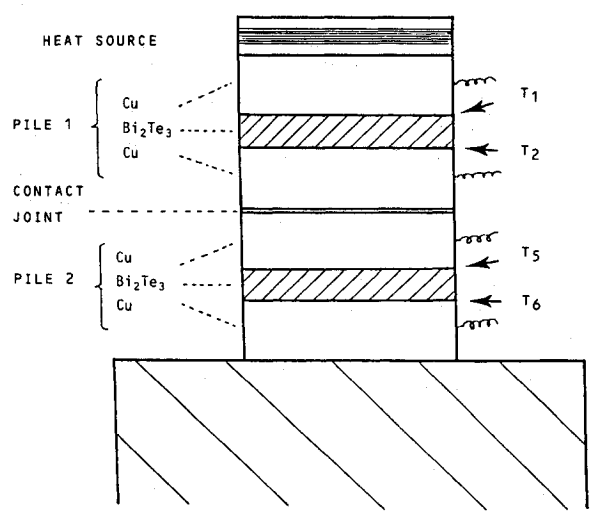

Fig. 4 Experimental device.

Table 1 Experimental test conditions

Test number	Roughness, m	Mechanical load Pa	Interstitial air pressure Pa
0	2×10^{-6}	10^6	Grease
1	2×10^{-6}	5×10^5	10^5
2	2×10^{-6}	2×10^5	10^5
3	10^{-5}	2×10^5	10^5
4	10^{-5}	3×10^5	10
5	10^{-5}	2×10^5	10

Table 2 Amplitude A and phase φ for various frequencies f and signals

f, mHz	20 A	20 φ,°	60 A	60 φ,°	100 A	100 φ,°
Sinusiodal	0.419	72.6	0.141	109.5	0.074	131.0
Square harmonic 1	0.407	73.2	0.140	113.8	0.074	137.0
Square harmonic 3	0.407	72.3	0.143	115.0	0.071	135.0

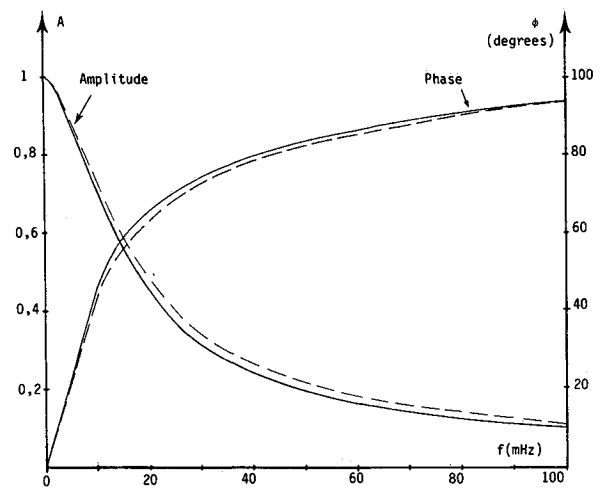

Fig. 5 Comparison between theory and experiments for perfect contact joint.

2) The frequency of the signal lies between 0.001 and 0.3 Hz.

3) The signal is either sine or square shaped.

The five experimental tests are summarized in Table 1. In order to verify the model developed for this experiment and to prevent from systematic errors, a perfect contact joint is first studied using samples of low roughness (2×10^{-6} m) under high mechanical load (10^6 Pa) and the interstitial air being replaced by grease (test number 0).

Figure 5 shows a very good agreement between model and experiment for the whole frequency range. This agreement justifies the assumption of perfect contact joints between the copper parts and the Bi_2Te_3 layers.

The linearity of the system has also been tested by comparison between sine and square transient measurements. In order to proceed to a conclusive experiment, it is necessary to use a "bad" contact so that its influence is the determining factor. A weak pressure contact (1.5×10^5 Pa) and a great size roughness (height greater than 10^{-5} m) have been chosen. The measurements have been made with various frequencies ($20 \leq f \leq 100$ mHz) with either a sinusoidal signal or the harmonics 1 and 3 of a square signal. The results (amplitude A and phase φ) are presented in Table 2. They clearly demonstrate the linearity of the phenomenon.

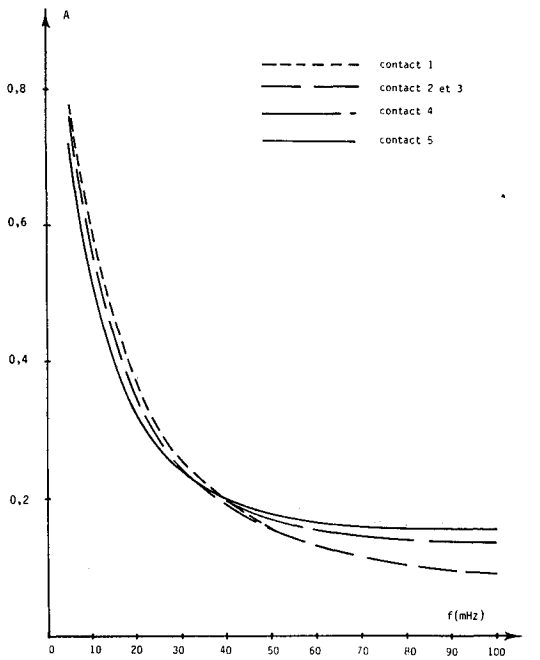

a) experimental results

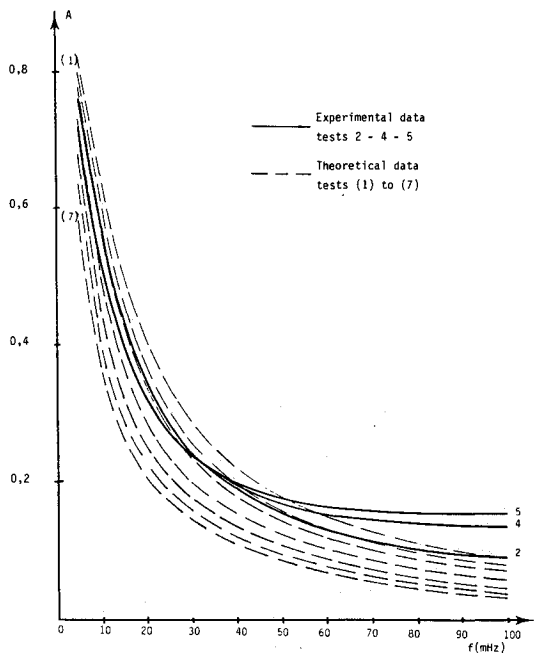

b) comparison between theoretical and experimental results for a real contact

Fig. 6 F_2/F_1 amplitude.

C. Comparison with Theory

Figures 6 and 7 compare the experimental results to the theoretical ones obtained with a purely resistive contact model for different values of the contact resistance R_c [(1): $R_c = 0$; (2): $R_c = 10^{-4}$; (3): $R_c = 2 \times 10^{-4}$; (4): $R_c = 4 \times 10^{-4}$; (5) $R_c = 6 \times 10^{-4}$; (6) $R_c = 8 \times 10^{-4}$; (7) $R_c = 10^{-3}$ $Km^2 W^{-1}$]. The agreement is good in the 0–0.02 Hz range, which confirms the results from literature. Beyond 0.02 Hz, theory and experiments differ significantly; the most surprising result is that theoretical and experimental amplitude curves intersect for the value of 0.04 Hz; at 0.1 Hz, a worse contact will be the cause of a higher amplitude.

The pure resistive model did not compare well with the experimental results. The results of the model developed in Sec. II are therefore compared with the experimental data.

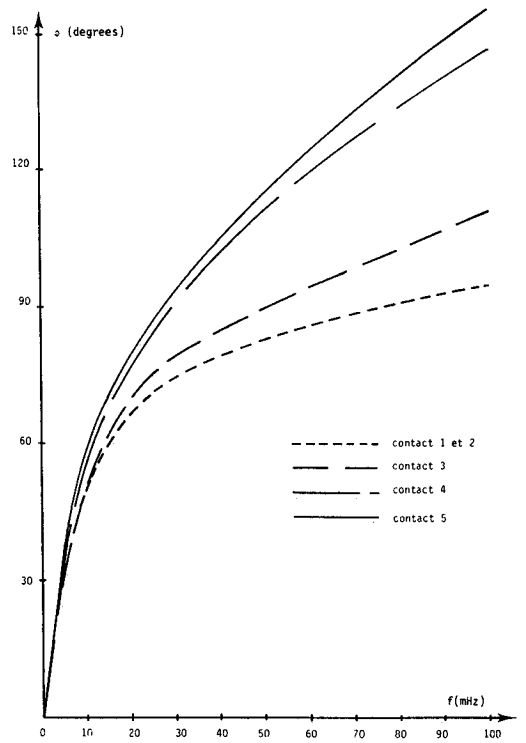

a) experimental results

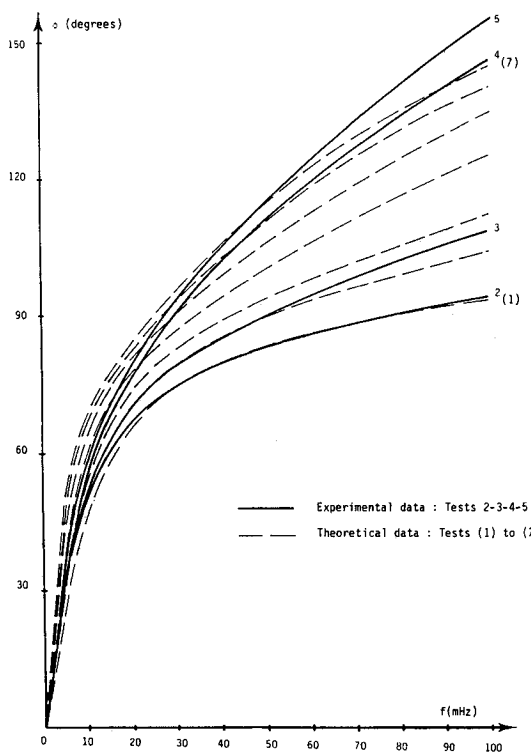

b) comparison between theoretical and experimental results for a real contact

Fig. 7 F_2/F_1 phase angle.

The chosen data for the contact joint are $\lambda = 395$ W m^{-1} K^{-1}; $a = 1.14\ 10^{-4}$ m^2 s^{-1}; $R = 10^{-4}$ m; $s/S = 10^{-3}$; $\delta = \delta_1 + \delta_2 = 10^{-5}$ m, where δ is the spot thickness.

These values qualify rather large contact spots. The constriction impedance takes the form

$$Z_c \simeq 2.2\ 10^{-4}\,[1 - 10^{-2}\sqrt{f}\,(1 + i)](\text{K m}^2\ \text{W}^{-1}) \quad (33)$$

For frequencies below 1 Hz, calculations lead to the quadripole

$$A = D \simeq 1$$

$$B \simeq 2.1\ 10^{-4}\ \text{K W}^{-1}\ \text{m}^2$$

$$C \simeq 0.34\,fi\ \text{W m}^{-2}\ \text{K}^{-1} \quad (34)$$

The constriction impedance Z_c is almost identical to a thermal resistance. A capacitive term (C) appears which modifies the pure resistive model. In fact, this term has no influence on the theoretical curves (within a relative error of 10^{-4}). For higher frequencies, it would increase the phase angle, which is in accordance with the experimental data, but would decrease the amplitude, which contradicts the experiments. Our model is then unable to explain the data obtained for frequencies higher than 0.02 Hz.

These quite surprising results are yet unexplained. The deviations could be due to thermoelastic effects—the contact geometry may be altered with time—or to heat and mass transfer effects—evaporation and condensation phenomena at the contact spots scale. But the perfect linearity of the system has to be outlined also.

IV. Experiments on Macro-Contact Joint

The foregoing experiments have shown that the concept of a pure thermal resistance does not work for frequencies lower than 0.02 Hz. The theoretical model developed is Sec. II.C is almost identical to a pure resistance for frequencies lower than 1 Hz. So, in order to test the validity of this model, it is necessary to change the characteristic time of the contact spot, that is to say to increase the value of r_0^2/a as it is easily verified in Eq. (25).

That is the reason why a new measurement setup which may work either in steady state or in steady periodic state on a macroscopic contact unit cell has been built.

A. Experimental Setup

The experimental setup is described in Fig. 8; it is composed of a heat source, a heat sink (regulated waterbox), two fluxmeters and the contact cell.

The latter is made of a brass cylinder with a groove simulating a single contact. With such a system, it is possible to calculate the theoretical quadripole associated to the contact joint and to show up the influence of the constriction impedance for lower frequencies than in the real contact case.

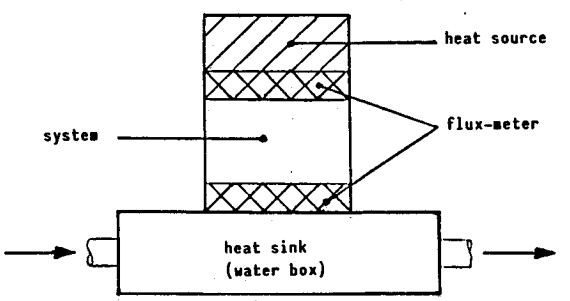

a) experimental setup

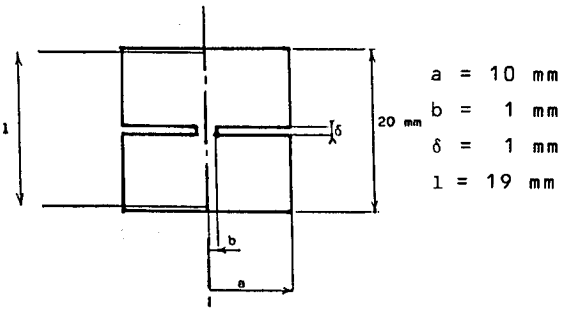

b) macro-contact cell

Fig. 8 Macro-contact joint.

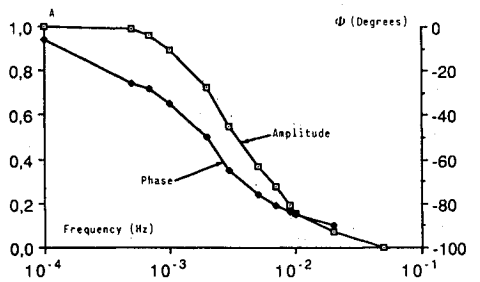

a) theoretical curves

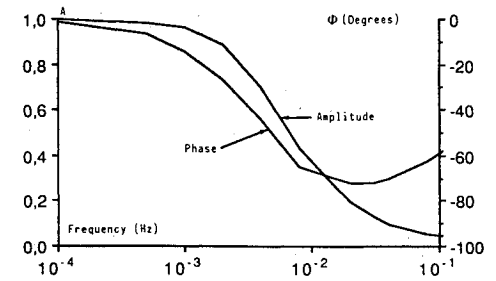

b) experimental curves

Fig. 9 Generalized impedance for a macro-contact joint.

The measurement device is composed of two thermocouples and two flux-meters to measure the heat transfer in and out of the cylinder.

B. Results in Steady State

Depending on the assumptions on the boundary conditions at the contact spot (uniform heat flux density or uniform temperature), theoretical calculations yield an overall thermal resistance of 7.8 K W^{-1} or 7.1 K W^{-1}; measurement (numerous and difficult) give 7.1 ± 0.7 K W^{-1}. This good agreement confirms the significance of this type of experiment.

C. Results in Sine State and Comparison with Theory

Being able to measure both temperatures and heat fluxes in and out of the system, it is then possible to identify all terms of the quadripole (A, B, C, and D). The observed parameter of the system is its generalized thermal impedance z_g defined by:

$$T_1 - T_2 = z_g \cdot \frac{\Phi_1 + \Phi_2}{2} \tag{35}$$

where T_1, T_2 are the input and the output temperatures, Φ_1, Φ_2 the input and output heat fluxes. In steady-state conditions $\Phi_1 = \Phi_2$ and z_g is equal to the thermal resistance of the system.

From a theoretical point of view, z_g is given by:

$$z_g = 2 \cdot \frac{A - 1}{C} \tag{36}$$

In the particular case of macro-contact joint, the theoretical modulus and phase of z_g are shown in reduced form (with respect to the steady-state thermal resistance) in Fig. 9a.

For frequencies greater than 0.001 Hz, the macro-contact does not behave like a resistance; this phenomenon appears on real contact joints for frequencies greater than 1 Hz, which is very difficult to obtain experimentally; this result justifies the present study of a macro-contact joint (artificial contact).

On Fig. 9b are shown the experimental data for this system; a good accordance is obtained between theory and experiment, which confirms the theoretical analysis given in Sec. II.

V. Conclusion

From the theoretical point of view, a model of thermal contact resistance has been developed in transient state. Based on a cylindrical unit cell, it takes into account both the setting up of the heat flux lines ("constriction" quadripole) and the thermal capacities of the contact spots and of the interstitial fluid ("wall" quadripole).

On a macro-contact joint simulating a real contact on a unit cell, the agreement between theory and experiment is good. Some careful experiments have been carried out on real contacts. They demonstrate the linearity of the heat transfer even in unsteady-state conditions. But neither the classical pure resistive model nor this new model are able to explain the deviation between theory and experiment observed in the 20–100 mHz frequency range.

Appendix: Constriction Impedance for a Semi-Infinite Medium

Using the scheme of Fig. 2b, the problem is written

$$\frac{1}{a}\frac{\partial T}{\partial t} = \frac{1}{r}\frac{\partial}{\partial r}\left(r\frac{\partial T}{\partial r}\right) + \frac{\partial^2 T}{\partial z^2} \tag{A1}$$

with the following boundary conditions ($t > 0$)

$$x = 0 \qquad \frac{\partial T}{\partial x} = -\frac{q}{\lambda} \qquad 0 < r < r_0$$
$$= 0 \qquad r_0 < r \tag{A2}$$

$$x \to \infty \qquad T = 0 \tag{A3}$$

and the initial condition

$$\text{at } t = 0 \qquad T = 0 \tag{A4}$$

Use of Laplace transform with the initial condition (A4) leads to

$$\frac{p}{a}\theta = \frac{1}{r}\frac{\partial}{\partial r}\left(r\frac{\partial \theta}{\partial r}\right) + \left(\frac{\partial^2 \theta}{\partial z^2}\right) \tag{A5}$$

Variables separations with the boundary condition (A3) yields to

$$\theta = \int_{\alpha=0}^{\infty} A(\alpha) J_0(\alpha r) \exp(-\gamma x)\, d\alpha \tag{A6}$$

with

$$\gamma^2 = \alpha^2 + p/a \quad (\alpha \text{ and } \gamma > 0)$$

Use of the boundary condition (A2) where the heat flux q (and so its Laplace transform φ) is uniform and of Hankel transform gives

$$A(\alpha) = \frac{\varphi}{\gamma}\frac{r}{\lambda} J_1(\alpha r_0) \tag{A7}$$

and therefore

$$\theta = \frac{\varphi r_0}{\lambda} \int_{\alpha=0}^{\infty} \frac{1}{\gamma} J_1(\alpha r_0) J_0(\alpha r) \exp(-\gamma x)\, d\alpha \tag{A8}$$

The average temperature $\bar{\theta}$ over the circular area ($x = 0$; $r < r_0$) is easily calculated:

$$\bar{\theta} = \frac{1}{r_0^2}\int_0^{r_0} \theta 2r\, dr = \frac{2\varphi}{\lambda}\int_{\alpha=0}^{\infty} \frac{J_1^2(\alpha r_0)}{\alpha\gamma}\, d\alpha \tag{A9}$$

The constriction impedance is then defined by:

$$z_c = \frac{\bar{\theta}}{\Phi} = \frac{\bar{\theta}}{\pi r_o^2 \varphi} = \frac{2}{\pi \lambda r_0} \int_{\varepsilon=0}^{\infty} \frac{J_1^2(\varepsilon)}{\varepsilon \sqrt{\varepsilon^2 + \frac{p r_0^2}{a}}} \, d\varepsilon \quad \text{(A10)}$$

References

[1]Bardon, J. P., Cassagne, B., Faucher, B., and Saint-Blanquet, C., "Bilan des Principales Recherches sur les Resistances Thermiques de Contact," Rept. D.E.T.B. 7101, March 1971.

[2]Bardon, J. P., "Introduction à l'Étude des Résistances Thermiques de Contact," *Revue Générale de Thermique Française,* Vol. XI, No. 125, 1972, pp. 429–447.

[3]Madhusudana, C. V., and Fletcher, L. S., "Contact Heat Transfer—the Last Decade," *AIAA Journal,* Vol. 24, No. 3, 1986, pp. 510–523.

[4]Fletcher, L. S., "Recent Developments in Contact Conductive Heat Transfer," *Journal of Heat Transfer,* Vol. 110, Nov. 1988, pp. 1059–1070.

[5]Doin, Y., "Contribution à l'Étude des Contacts Solide-Solide en Régimes Variables," Doctoral Dissertation, Instit. National Polytechnique de Lorraine, Nancy, 1986.

[6]Carslaw, H. S., and Jaeger, J. C., "Conduction of Heat in Solids," 2nd ed., Oxford University Press, Oxford, England, 1959.

[7]Bardon, J. P., "Aspect Thermocinétique des Erreurs de Mesure de Température par Contact," Comptes Rendus Scientifiques du Groupement Univ. Thermique, 1975.

[8]Degiovanni, A., and Moyne, C., "Résistance Thermique de Contact en Régime Permanent: Influence de la géométrie du Contact," *Revue Générale de Thermique Française,* No. 334, 1989, pp. 557–564.

[9]Degiovanni, A., Sinicki, G., Gery, A., and Laurent, M., "Un Modèle de Résistance Thermique de Contact en Régime Permanent," *Revue Générale de Thermique Française,* No. 267, March 1984, pp. 161–175.

[10]Degiovanni, A., "Conduction dans un Mur Multicouche avec Sources: Extension de la Notion de Quadripôle," *International Journal of Heat and Mass Transfer,* Vol. 31, No. 3, 1988, pp. 553–557.